Hierarchy of Bound States in the One-Dimensional Ferromagnetic Ising Chain $CoNb_2O_6$ Investigated by High-Resolution Time-Domain Terahertz Spectroscopy

C. M. Morris,[1] R. Valdés Aguilar,[1,2] A. Ghosh,[1] S. M. Koohpayeh,[1] J. Krizan,[3] R. J. Cava,[3] O. Tchernyshyov,[1] T. M. McQueen,[1,4] and N. P. Armitage[1]

[1]*The Institute for Quantum Matter, Department of Physics and Astronomy, The Johns Hopkins University, Baltimore, Maryland 21218, USA*

[2]*Center for Integrated Nanotechnologies, Los Alamos National Laboratory. MS K771. Los Alamos, New Mexico 87545, USA*

[3]*Department of Chemistry, Princeton University, Princeton, New Jersey 08544, USA*

[4]*Department of Chemistry, The Johns Hopkins University, Baltimore, Maryland 21218, USA*

(Received 3 October 2013; published 2 April 2014)

Kink bound states in the one-dimensional ferromagnetic Ising chain compound $CoNb_2O_6$ have been studied using high-resolution time-domain terahertz spectroscopy in zero applied magnetic field. When magnetic order develops at low temperature, nine bound states of kinks become visible. Their energies can be modeled exceedingly well by the Airy function solutions to a 1D Schrödinger equation with a linear confining potential. This sequence of bound states terminates at a threshold energy near 2 times the energy of the lowest bound state. Above this energy scale we observe a broad feature consistent with the onset of the two particle continuum. At energies just below this threshold we observe a prominent excitation that we interpret as a novel bound state of bound states—two pairs of kinks on neighboring chains.

DOI: 10.1103/PhysRevLett.112.137403 PACS numbers: 78.30.Hv, 75.30.-m, 76.50.+g

The one-dimensional Ising spin chain is a paradigmatic example of an interacting quantum many body system. Its low dimensionality increases its propensity for quantum fluctuations and hence its tendency to exhibit interesting quantum effects. It has been proposed to host a number of exotic states of matter including ones with fractional excitations and novel quantum critical points (QCPs) [1–4]. Moreover, the one-dimensionality often makes a theoretical formulation more tractable and a direct comparison between experiment and theory possible.

Recently, the Ising spin chain compound $CoNb_2O_6$ has been of interest due to a fascinating set of neutron scattering experiments performed by Coldea *et al.* [5]. By applying a magnetic field transverse to the 1D ferromagnetic spin chains, they were able to tune through a QCP from a spin-ordered phase to a paramagnetic state. At the QCP near 5.5 T they observed that the ratio of energies of the two lowest lying magnetic excitations was the golden ratio. This was consistent with an emergent E8 symmetry at the transverse field-tuned QCP predicted by Zamolodchikov [4] for an Ising chain in the presence of a weak longitudinal field.

Ising spin chains also show interesting behavior in the absence of a transverse field when a weak longitudinal field is present. At zero field the linear ferromagnetic Ising chain has a twofold degenerate ground state. For an isolated chain, the excitations are sets of n flipped spins, called "spin clusters" [6,7]. For pure Ising interactions, domains of different length are degenerate, as the exchange interaction is only broken at the ends of the cluster in domain walls or "kinks" [8,9]. A longitudinal field lifts the degeneracy of domains of different length, with the energy to create longer chains increasing linearly with the separation between kinks. Small interactions beyond pure Ising allow the kinks to move. McCoy and Wu [2] solved for the excitations in this model, where two kinks can be treated as two particles moving in one dimension with a confining potential $\lambda|x|$ between them. In the continuum approximation the discrete nature of the spin chain can be ignored and the center-of-mass motion of the kinks can be described by a Schrödinger equation

$$-\frac{\hbar^2}{\mu}\frac{d^2}{dx^2}\psi(x) + \lambda|x|\psi(x) = (m - 2m_0)\psi(x). \quad (1)$$

Solutions to this equation are Airy functions with energy eigenvalues of the kink bound states [2]

$$m_n = 2m_0 + z_n\lambda^{2/3}\left(\frac{\hbar^2}{\mu}\right)^{1/3}, \qquad n = 1, 2, 3\ldots, \quad (2)$$

where m_n is the bound state energy, m_0 is the energy to break the nearest neighbor exchange interaction, λ is proportional to the longitudinal magnetic field, and the z_n's are the negative zeros of the Airy function of the first kind. In $CoNb_2O_6$, antiferromagnetic (AF) ordering of ferromagnetic chains below 1.97 K produces a weak effective longitudinal mean field. In their neutron scattering measurements Coldea *et al.* found a sequence of five bound states that correspond to the first five solutions of this Airy function model [5]. One can make an analogy between the linear confining potential and confinement in quantum

chromodynamics, where a kink plays the role of a quark with bare mass m_0 and the kink bound state plays the role of a meson. This analogy has been made recently for spin ladders [10].

In addition to neutron studies, insight into similar materials has been gained using far infrared light as a probe. Torrance and Tinkham [6,7] did pioneering work on one-dimensional Ising chains, looking at $CoCl_2 \cdot 2H_2O$ using a far-infrared grating spectrometer. They developed a model of the spin cluster excitations based on Ising basis functions, calculating the energies of discrete spin flip transitions in a strong longitudinal field. In $CoNb_2O_6$, some preliminary work was done using Fourier transform infrared spectroscopy and electron spin resonance [11,12]. However, the resolution was too low to resolve the excitations predicted by Eq. (1).

In this Letter we use high-resolution time-domain terahertz spectroscopy (TDTS) to investigate these kink excitations in $CoNb_2O_6$ in the far infrared. The high signal-to-noise ratio, excellent energy resolution, and short acquisition times of the technique allow us to find a number of excitations that were previously unresolved by neutron scattering. In addition to the five kink bound states observed by Coldea *et al.* [5], terahertz spectroscopy shows a further four kink bound states and a new higher energy excitation below the continuum that we interpret as a bound state of bound states.

$CoNb_2O_6$ belongs to the orthorhombic *Pbcn* space group. Crystal field splitting produces an effective spin $1/2$ moment on the Co^{+2} ions, with the spins lying in the *ac* plane at an angle of $\pm 31°$ to the *c* axis [13,14]. The Co atoms form zigzag chains along the *c* axis. Ferromagnetic exchange interactions between nearest-neighbor Co^{+2} ions along this axis cause ferromagnetic correlations in these chains beginning at ~25 K [15]. Below 2.95 K weak AF interchain exchange interactions stabilize a spin-density wave along the *b* direction with a temperature-dependent ordering wave vector *Q*. Below 1.97 K the spin-density wave becomes commensurate AF along *b* with a temperature independent $Q_{\mathrm{AF}} = (0, 1/2, 0)$ and an ordered moment of $3.05\mu_B$ [16]. As mentioned above, in this low temperature phase the effects of weak interchain couplings can be understood as a small effective longitudinal field that scales with the ordered moment.

The $CoNb_2O_6$ samples used here were grown by the floating zone method and characterized by powder and back-reflection x-ray Laue diffraction. The samples were small discs approximately 5 mm in diameter and 600 μm thick. TDTS [17,18] was performed (Fig. 1) using a home-built transmission mode spectrometer that can access the electrodynamic response between 100 GHz and 2 THz (0.41–8.27 meV). Taking the ratio of the transmission through a sample to that of a reference aperture gives the complex transmission coefficient (see the Supplemental Material [19] for further details). The electric and magnetic fields of the terahertz waveform can be used to probe both electric and magnetic dipole excitations in the material. In the present case of magnetic insulators the time-varying magnetic field of the pulse couples to the spins of the system, essentially equivalent to frequency domain electron spin resonance. As the wavelength of terahertz range radiation is much greater than typical lattice constants (1 THz ~ 300 μm), TDTS measures the $q \to 0$ response. The complex transmission $T(\omega)$ is related to the complex susceptibility $\chi(\omega)$ at $q = 0$ as $-\ln(T(\omega)) \propto \omega\chi(q = 0, \omega)$.

In Fig. 2(a) we show the absorption spectra (wave vector $\mathbf{k} \| c$, and ac electric and magnetic fields $\mathbf{e} \| a$ and $\mathbf{h} \| b$) down to temperatures just above the 2.95 K transition to the incommensurate ordered state. In this orientation, three features develop as the temperature is lowered: a low energy peak at 300 GHz, a higher energy peak at 500 GHz, and a broad background excitation we call the continuum. We label the 300 GHz peak the *m* excitation and the 500 GHz peak the $2m$ excitation for reasons explained below. To determine whether the observed excitations are electric or magnetic dipole active, a full polarization dependence study was performed on three samples in a total of six orientations, the results of which are detailed in Table I. The observed excitations correlate with the ac magnetic field direction, and are therefore magnetic dipole active. As Fig. 2(a) shows, the absorption strength of these transitions increases with decreasing temperature. This temperature dependence is consistent with the onset of ferromagnetic correlations in the chains along the c axis near 25 K [15].

To understand the origin of the excitations, a magnetic field dependence experiment was performed at 6 K, above all interchain ordering transitions, but well below the temperature where strong ferromagnetic correlations develop along chains. The magnetic field was applied along the *a* axis, with the terahertz waveform oriented with $\mathbf{k} \| a$, $\mathbf{e} \| c$, and $\mathbf{h} \| b$, the Faraday geometry. In this configuration, the *m*, $2m$, and continuum excitations are all observed at zero field. As Figs. 2(b) and 2(c) show, the *m* and $2m$ peaks split, as predicted by the theory of Torrance and Tinkham for spin chains in a pure longitudinal field [6]. The slope of the lines is proportional to the total spin in the

TABLE I. Polarization dependence of the absorption peaks at $T = 3$ K. An *x* indicates the observed presence of the feature for the particular terahertz polarization condition.

Polarization	*m*	$2m$	Continuum
$h\|\|a, e\|\|b$		x	x
$h\|\|a, e\|\|c$		x	x
$h\|\|b, e\|\|a$	x	x	x
$h\|\|b, e\|\|c$	x	x	x
$h\|\|c, e\|\|a$	x		
$h\|\|c, e\|\|b$	x		

excited state. In the present case their zero field intercept reflects the number of kink pairs in the excited state. The m peak splits into a one–spin flip excitation labeled $m1$, and a two–spin flip excitation $m2$. The $2m$ peak splits into a $2m1$ excitation with the same slope as $m2$ (e.g., a two–spin flip state) and a three–spin flip $2m2$ excitation. From the zero field intercepts of these excitations [6], we assign $m1$ and $m2$ as two kink excitations and the $2m1$ and $2m2$ as four kink excitations.

In the commensurate state below 1.97 K, the spin flip excitations should resolve into a series of bound state excitations as the effective longitudinal field from interchain interactions introduces an effective attraction between the kinks. The energy between these subdivided excitations is expected to be on the order of 0.1 meV (24 GHz). In TDTS the total time scanned determines the spectral resolution. In further measurements the delay stage was scanned 9 mm (~60 ps), giving an energy resolution of 0.07 meV (17 GHz). However, increasing the measured terahertz pulse duration complicates the analysis, as multiple reflections in the crystal are now observed [Fig. 1]. These give pronounced Fabry-Perot resonance peaks at frequencies where half integral wavelengths of light fit inside the sample. These resonance peaks could not be numerically removed sufficiently for the magnetic peak structure to be discerned. We instead use a new technique to extract high-resolution spectra of magnetic excitations obscured by Fabry-Perot oscillations. First, the low temperature spectra are referenced to high-resolution spectra at 3.0 K just above the interchain ordering temperature. Assuming a constant index of refraction between these two temperatures, the Fabry-Perot resonances cancel. By further referencing to a temperature above the ferromagnetic chain ordering, the absorption due to magnetic transitions alone can be isolated. This analysis is described in detail in the Supplemental Material [19].

Figure 3(a) shows the result of this normalization for the high-resolution spectrum at 1.6 K. The broad absorption seen at higher temperatures subdivides into a dramatic structure of peaks. At the lowest energies, a series of nine

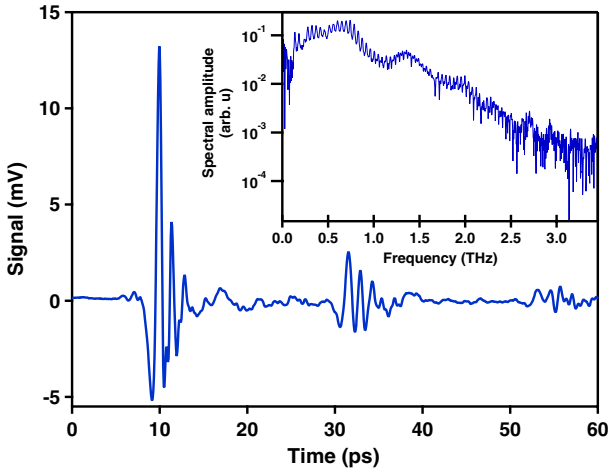

FIG. 1 (color online). Sample waveform at 5 K for $\mathbf{k}\|b$, $\mathbf{e}\|c$, $\mathbf{h}\|a$. Fine features in the spectral amplitude below 2.5 THz are not due to noise, but rather Fabry-Perot oscillations caused by the multiple reflections of the time domain pulse in the $CoNb_2O_6$ crystal.

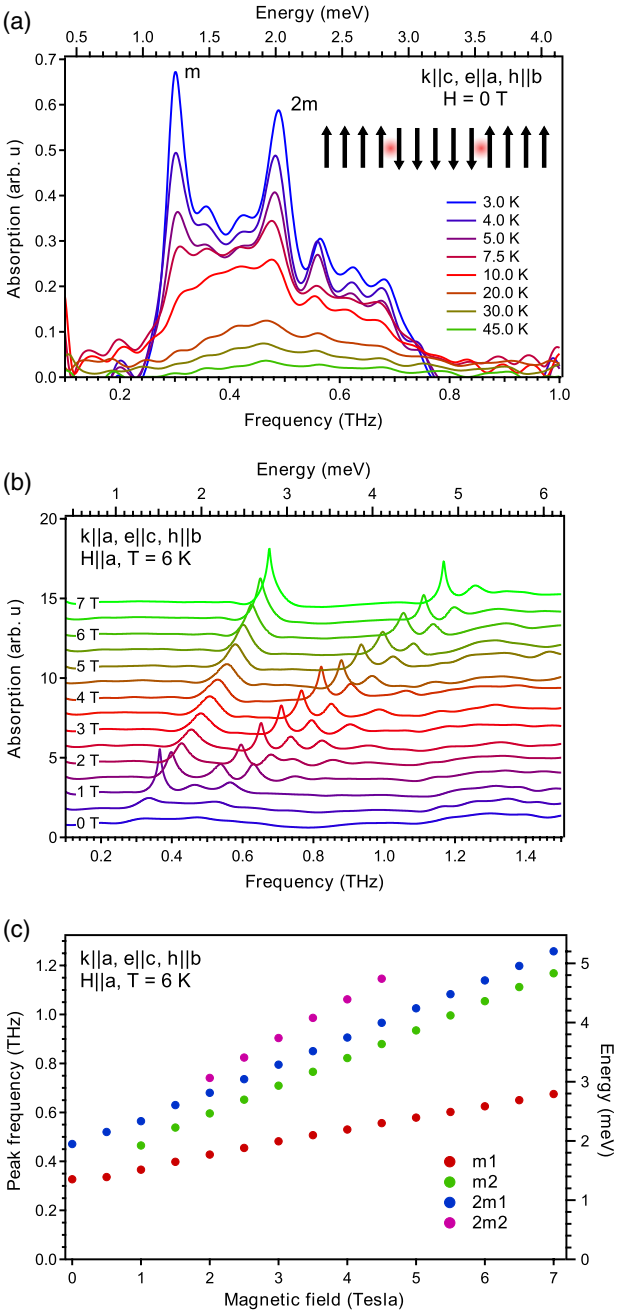

FIG. 2 (color online). (a) $\mathbf{k}\|c$, $\mathbf{e}\|a$, $\mathbf{h}\|b$ absorption above the incommensurate ordering temperature 2.95 K parallels the development of ferromagnetic correlations in the chains. The inset shows a five-spin flip excitation above this ordering temperature, with kinks represented by red circles. (b) Magnetic field dependence for $\mathbf{k}\|a$, $\mathbf{e}\|c$, $\mathbf{h}\|b$ at 6 K. (c) Peak positions for $\mathbf{k}\|a$, $\mathbf{e}\|c$, $\mathbf{h}\|b$ at 6 K. H denotes the direction of the dc magnetic field.

peaks ($m1 - m9$) is observed, with intensity that decreases with increasing frequency. This series terminates with a more prominent peak at 500 GHz and is then followed by a broad continuum. As shown in Fig. 3(b) the energies of all nine of the lowest excitations can be described exceedingly well by the energies of the linearly confined kink model in Eq. (2). Our five lowest peaks have the same energies as the peaks seen in Ref. [5] at zero external field. We identify the broad feature as the onset of the two bound state continuum at an energy that is somewhat below the energy of $m1 + m1$. The fact that no kink bound states are observed above the threshold shows the utility of the quark confinement analogy. Free kinks (quarks) are impossible because above a threshold energy of twice the lowest bound state energy $m1$, it is energetically more efficient to excite two kink bound states $m1 + m1$ (two pairs of quarks). As discussed below, we believe the large peak ($2m1$) below the onset of the continuum is a bound state of two $m1$ kink bound states on adjacent chains. We are able to resolve additional excitations beyond those observed by Coldea *et al.* [5] due to the high signal-to-noise ratio of TDTS and its relative weighting of the absorption spectra over $\chi(\omega)$ by a factor of ω. This highlights the utility of TDTS as a complementary high-resolution technique for magnetic systems.

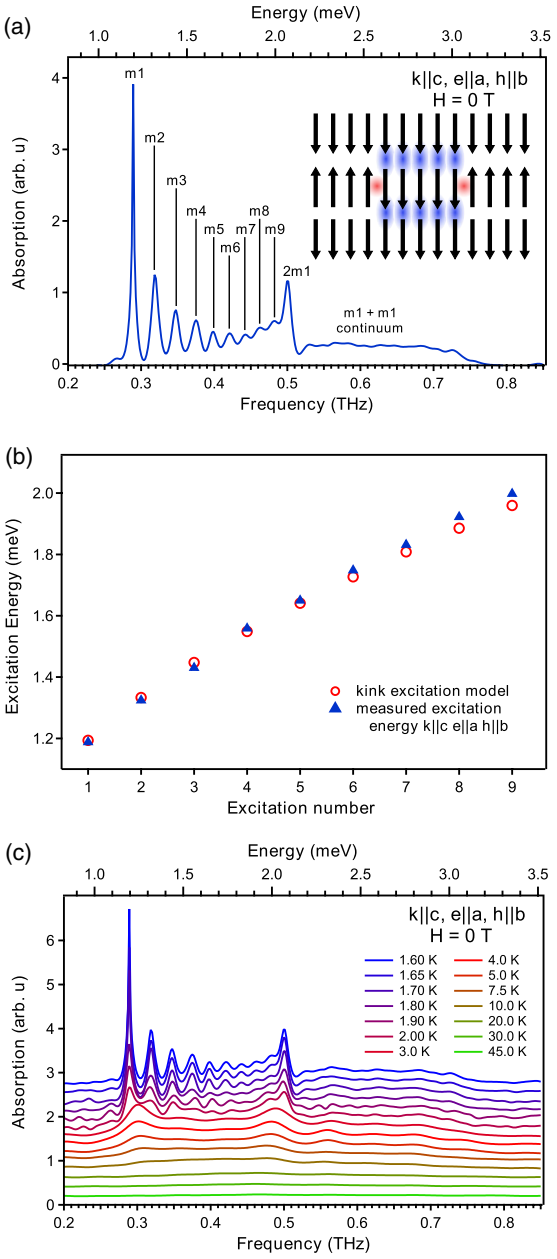

FIG. 3 (color online). (a) 1.6 K high-resolution scan showing the hierarchy of excitations ($m1 - m9$), the $2m1$ excitation, and the continuum. The inset shows a five-spin flip excitation, where the red circles represent kinks on a single chain, and the blue circles show where the antiferromagnetic interchain order in the b direction is broken. The exact intensity and line shape of the $m1$ peak is difficult to determine, as at this frequency nearly all of the light was absorbed. (b) Comparison of the energies predicted by Eq. (2) and the energies in (a). Error bars are within the width of the markers. (c) High resolution temperature dependence, showing that the kink bound states disappear as the interchain ordering is lost at ~3 K.

The temperature dependence of these excitations is shown in Fig. 3(c). At temperatures well below the ordering at 1.97 K, the excitations are well defined. As the temperature increases, they become less prominent. As the ordering changes from commensurate to incommensurate AF near 2 K, the peaks become barely resolvable. Above the incommensurate ordering at 3 K, we see that they have reduced to their higher temperature behavior. We see that the series of sharp peaks ($m1 - m9$) evolves out of the high temperature m peak and the $2m1$ peak evolves out of the $2m$ peak.

Finally, we look at the $2m1$ peak at 500 GHz, which is associated with four kinks, i.e., two separate spin clusters. The energy of the peak is well below what one would expect for two isolated $m1$ excitations, which would appear at 580 GHz for the observed $m1$ excitation frequency of 290 GHz. Instead, the $2m1$ excitation appears near 500 GHz. This, and its sharpness, implies that it is associated with a bound state, as the two particle excitations give rise to the continuum. We note that upon close inspection this feature can be seen in the data of Coldea *et al.* [5] where it appears as a dispersionless mode. The most obvious source for binding between $m1$ excitations would come from two single spin flip excitations on adjacent chains. A simple classical model for paired bound states without relative motion gives a rough estimate for the $2m1$ frequency of 532 GHz. This is based on a modified version of Eq. (2) where one pays an energy cost $4m_0$, but only half the interaction energy per kink pair due to the fact that the spin flips are on adjacent chains.

To further investigate the $2m1$ excitation, numerical calculations were performed that predict the existence of a bound state between $m1$ excitations on adjacent chains in a manner proposed above. With the accepted parameters for $CoNb_2O_6$ the energy of this bound state was calculated to be 564 GHz, lying below the calculated bottom of the

$m1 + m1$ continuum at 2×286 GHz $= 572$ GHz. While the quantitative agreement is not exact, qualitatively the existence of a bound state below the continuum is confirmed. Moreover, calculated dispersion curves show that the $2m1$ mode has a significantly reduced dispersion compared to the $m1$ state, although again the calculated dispersion is not as flat as that observed by Coldea *et al.* Consistent with observation, the spectral weight in this novel excitation is predicted to be appreciable and of order the weight in the $m2$ peak. See the Supplemental Material [19] for further details.

We have reported the observation of nine kink bound states in the one-dimensional spin chain $CoNb_2O_6$ by high resolution-time-domain terahertz spectroscopy. Their energies can be modeled exceedingly well by the Airy function solutions to a 1D Schrödinger equation in a linear confining potential. This sequence of bound states terminates at a threshold energy 2 times the lowest bound state energy. Above this energy scale we observe a broad feature consistent with the onset of the two particle continuum. At energies just below this threshold we observe a prominent excitation at an energy somewhat less than 2 times the lowest bound state. We interpret this feature as resulting from a novel bound state of bound states on neighboring chains. These results highlight the complementary role that terahertz spectroscopy can play to neutron studies of magnetic systems.

We would like to thank C. Broholm, I. Cabrera, J. Deisenhofer, J. Kjäll, J. Moore, K. Ross, and M. Mourigal for helpful discussions. The terahertz measurements and instrumentation development were funded by the Gordon and Betty Moore Foundation through Grant No. GBMF2628 to N. P. A. The crystal growth and theoretical work were funded by the DOE-BES through DE-FG02-08ER46544.

[1] B. G. Levi, Phys. Today **63**, 13 (2010).
[2] B. M. McCoy and T. T. Wu, Phys. Rev. D **18**, 1259 (1978).
[3] H. C. Fogedby, J. Phys. C **11**, 2801 (1978).
[4] A. B. Zamolodchikov, Int. J. Mod. Phys. A **04**, 4235 (1989).
[5] R. Coldea, D. A. Tennant, E. M. Wheeler, E. Wawrzynska, D. Prabhakaran, M. Telling, K. Habicht, P. Smeibidl, and K. Kiefer, Science **327**, 177 (2010).
[6] J. B. Torrance and M. Tinkham, Phys. Rev. **187**, 587 (1969).
[7] J. B. Torrance and M. Tinkham, Phys. Rev. **187**, 595 (1969).
[8] P. Pfeuty, Ann. Phys. (N.Y.) **57**, 79 (1970).
[9] S. Rutkevich, J. Stat. Phys. **131**, 917 (2008).
[10] B. Lake, A. M. Tsvelik, S. Notbohm, D. A. Tennant, T. G. Perring, M. Reehuis, C. Sekar, G. Krabbes, and B. Büchner, Nat. Phys. **6**, 50 (2009).
[11] T. Kunimoto, M. Sato, K. Nagasaka, and K. Kohn, J. Phys. Soc. Jpn. **68**, 1404 (1999).
[12] T. Kunimoto, K. Nagasaka, H. Nojiri, S. Luther, M. Motokawa, H. Ohta, T. Goto, S. Okubo, and K. Kohn, J. Phys. Soc. Jpn. **68**, 1703 (1999).
[13] C. Heid, H. Weitzel, P. Burlet, M. Bonnet, W. Gonschorek, T. Vogt, J. Norwig, and H. Fuess, J. Magn. Magn. Mater. **151**, 123 (1995).
[14] S. Kobayashi, S. Mitsuda, and K. Prokes, Phys. Rev. B **63**, 024415 (2000).
[15] T. Hanawa, K. Shinkawa, M. Ishikawa, K. Miyatani, K. Saito, and K. Kohn, J. Phys. Soc. Jpn. **63**, 2706 (1994).
[16] W. Scharf, H. Weitzel, I. Yaeger, I. Maartense, and B. Wanklyn, J. Magn. Magn. Mater. **13**, 121 (1979).
[17] R. Ulbricht, E. Hendry, J. Shan, T. F. Heinz, and M. Bonn, Rev. Mod. Phys. **83**, 543 (2011).
[18] M. Nuss and J. Orenstein, in *Millimeter and Submillimeter Wave Spectroscopy of Solids*, Topics in Applied Physics Vol. 74, edited by G. Grüner (Springer, Berlin Heidelberg, 1998), pp. 7–50.
[19] See Supplemental Material at http://link.aps.org/supplemental/10.1103/PhysRevLett.112.137403 for details of the terahertz spectroscopy and analysis, sample preparation, and theoretical calculations.